7th International Scientific Conference
Technics and Informatics in Education
Faculty of Technical Sciences, Čačak, Serbia, 25-27th May 2018

Session 3: Engineering Education and Practice
UDC: 530.1:004.42

A tomographic method for determining the distance between standing wave anti-nodes and the frequency of electromagnetic radiation inside a microwave oven

Milentije Luković [1*], Aleksandra Kalezić-Glišović[1], Borivoje Nedeljković[1], Sanja Antić[1]
[1] University of Kragujevac, Faculty of Technical Sciences Čačak, Serbia
[*] milentije.lukovic@ftn.kg.ac.rs

Abstract: *The paper identifies the challenges of the tomographic method for determining the position and shape of the modes of the electromagnetic standing wave in a microwave oven. The experiment described here shows the inhomogeneity of heating and unpredictability of the occurrence of anti-nodes, or hot-spots, inside the microwave oven chamber, as well as a procedure for their better localization. The proposed tomographic method has been used for characterizing and visualizing standing wave modes. As part of the described experiment, an algorithm is presented to determine the optimal dimensions of the 3D chamber, which represent a resonator where the standing wave is formed. Also, a mathematical procedure for calculating the radius of the circle through the circle chord is described in detail, which was used to determine the distance between two neighboring anti-nodes of the standing wave.*

Keywords: *standing wave; microwave oven; anti-nodes; hot-spots; circle chord*

1. INTRODUCTION

Microwave ovens are among the most common electrical appliances in households. However, their journey from discovery to acceptance by a wider audience lasted for quite a long time. Today, apart from food preparation, microwave ovens are also used in various branches of industry, science and medicine [1].

They can also be suitable teaching tools for demonstrating physico-chemical processes in various fields of applied physics [2], [3].

2. THEORY

The harmonic wave that moves in the positive direction of the x axis can be represented by the equation

$$y_1(x,t) = A\sin\left(\frac{2\pi x}{\lambda} - \omega t\right) \tag{1}$$

In the case of a reflection by a boundary placed on a side in the direction of wave propagation, it will be reflected and its direction and oscillation phase will change, so the equation of motion will then be

$$y_2(x,t) = A\sin\left(\frac{2\pi x}{\lambda} + \omega t\right) \tag{2}$$

As a result, a standing wave is created that represents the superposition of two waves $y_1(x,t)$ and $y_2(x,t)$, and the equation of the resulting wave will therefore read

$$y(x,t) = A\sin\left(\frac{2\pi x}{\lambda} - \omega t\right) + A\sin\left(\frac{2\pi x}{\lambda} + \omega t\right) \tag{3}$$

or otherwise written

$$y(x,t) = 2A\sin\left(\frac{2\pi x}{\lambda}\right)\cos(\omega t) \tag{4}$$

The last term describes a wave that oscillates in time and has a space dependence that is stationary [4]. At any point *x* the oscillation amplitude is constant and has a value $2A\sin\left(\frac{2\pi x}{\lambda}\right)$. The "nodes" of the standing wave are obtained for *x* values that correspond to even multiples of λ/4, and "anti-nodes" for odd multiples. In the nodes of the standing wave the sum of the amplitudes of the wave is zero, whereas in the anti-nodes it is maximal. Based on the above, it turns out that the distance between two nearby nodes (anti-nodes) of the standing wave is equal to λ/2 (Figure 1).

Constrained 3D space, such as the interior of a rectangular microwave oven, potentially represents a space where it is possible to form a standing wave [5]–[7]. Radiation inside the oven originates from a microwave radiation source named magnetron. The radiation reaches the food that needs to be heated by a special metal channel. Given the shape of the interior, which is as a rule square, and bearing in mind the fact that the walls are made of metal from which microwave radiation is reflected, the interior of the oven can be considered **as** a resonant cavity.

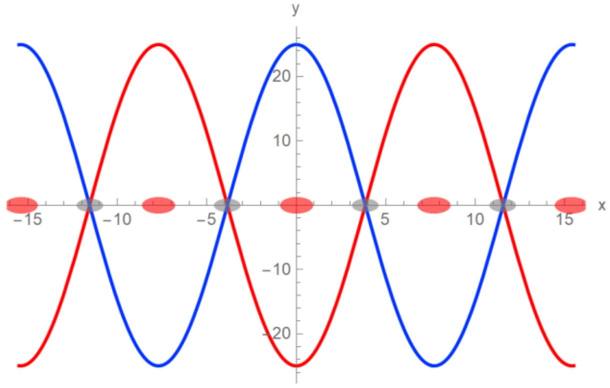

Figure 1. *Nodes and anti-nodes of the standing wave*

The resonant frequency, that is, the wavelength at which the formation of the standing wave will occur, depends on the internal dimensions of the resonator itself. The wavelength of the resonant frequency of the square-shaped resonators whose dimensions are L_x, L_y, L_z (Fig. 2), can be determined by the expression

$$\left(\frac{2}{\lambda}\right)^2 = \left(\frac{l}{L_x}\right)^2 + \left(\frac{m}{L_y}\right)^2 + \left(\frac{n}{L_z}\right)^2 \quad (5)$$

where l, m, n are positive integers (or zero) and represent the modes of the standing wave, and λ is the wavelength of the emitted electromagnetic radiation inside the oven [8].

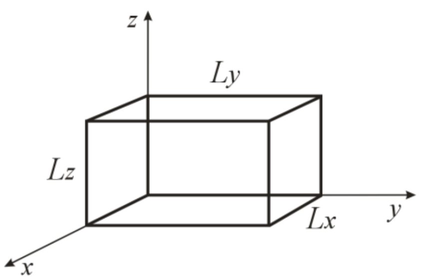

Figure 2. *Square-shaped resonator model*

If the dimensions of the oven chamber are such that they can be obtained as the product of an integer and the wavelength corresponding to the resonant frequency, then a 3D standing wave will be formed. The dimensions L_x, L_y, L_z of the chamber are proportional to the wavelength in each of the corresponding directions (x, y, z), that is

$$L_x = l\frac{\lambda_x}{2}, L_y = m\frac{\lambda_y}{2}, L_z = n\frac{\lambda_z}{2} \quad (6)$$

This means that λ_x, λ_y, λ_z are determined by the dimensions of the oven chamber, and expression (7) is obtained by replacing (6) in (5), [9]. Characteristic of equation (7) is that there are several solutions that correspond to resonant frequencies (wavelengths), which are in close proximity to the frequency (wavelength) of the radiation emitted by the magnetron

$$\frac{1}{\lambda^2} = \frac{1}{\lambda_x^2} + \frac{1}{\lambda_y^2} + \frac{1}{\lambda_z^2} \quad (7)$$

Various optimization algorithms can be used to find a solution to expression (7), which is overdetermined [10]. The approach we used to solve this problem was an algorithm written in Mathematica software, with certain limitations related to the range of values λ in which we sought the solutions. Given the fact that the emitted radiation frequency was υ_0 = 2.45 · 10^9 Hz, the exact wavelength (λ_0 = 12.236 cm) was obtained from c = λ · υ_0 (c = 2.997925 · 10^8 m/s). Therefore, the limit that we included in the calculation of modes (l, m, n) of the standing wave refers to the deviation of the wavelength in the interval from the exact value (i.e. 12 cm ≤ λ_0 ≤ 12.5 cm). The dimensions of the microwave oven at our disposal were: depth L_x = 25.5 cm, width L_y = 29.5 cm and height L_z = 18.1 cm. Consequently, the values of the oscillation modes (l, m, n) included in equation (1) were such that the wavelength λ_d in terms of value needed to be close to the wavelength of magnetron radiation λ_0 (Table 1).

Table 1. *Wavelengths λ_d whose values were close to the radiation wavelength of the magnetron λ_0, with relative errors and obtained oscillation modes for the microwave oven of dimensions L_x = 25.5 cm, L_y = 29.5 cm, L_z = 18.1 cm*

λ_d (cm)	δ_λ (%)	*l*	m	n
12.067	1.39	0	0	3
12.041	1.60	2	4	1
12.391	1.27	3	0	2
12.127	0.89	3	1	2
12.119	0.96	3	3	1
12.026	1.72	4	0	1
12.462	1.85	4	1	0

At first glance, the results obtained for the relative error of the wavelength of the emitted radiation (δ_λ) may appear quite small (<2%). Namely, from Table 1 shows that the smallest error for λ was obtained for mode $TE_{3,1,2}$ (TE - transverse electrics fields) and it was 0.89%. However, since the standing wave is formed on the basis of multiple reflections from the interior walls of the oven, it is obvious that the entered values of dimensions L_x, L_y, L_z did not entirely support its formation. The values of L_x, L_y, L_z were carefully selected to allow the radiation entering the oven interior to be as dispersed as possible, in order to make the food more efficiently and uniformly heated. Uneven heating in microwave ovens, since the time of its invention during the course the military research (in the Second World War) to the present day, when it represents a commercialized product, has never been completely eliminated. This phenomenon occurs even in modern devices, which is why an additional option has been implemented to eliminate this deficiency, which is based on the fact that during the heating process the body placed on the base (the bottom of the oven) is continuously rotated. Figure 3 shows thermal emission of electromagnetic radiation from the oven interior, on a square-shaped body. The image was taken using a thermal camera [11].

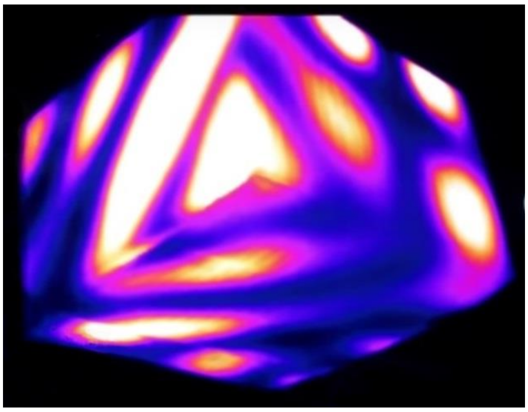

Figure 3. Thermal distribution of electromagnetic radiation on a stationary square-shaped body inside the oven [11].

In the case where the body does not rotate (as in Fig. 3), the anti-nodes of the standing wave (hot - bright areas) and the nodes (cold - dark areas) can be clearly seen with the thermal camera. They will be formed regardless of the fact that the very interior design attempted to minimize this phenomenon. Contrarily, better distribution of thermal energy can be achieved with rotation of the object inside the oven (Fig. 4) [11].

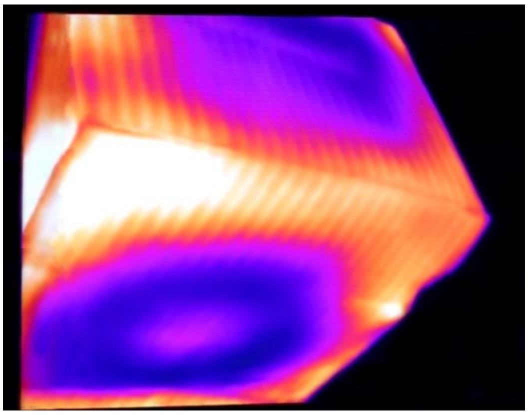

Figure 4. Thermal distribution of electromagnetic radiation on square-shaped body rotating inside the oven [11].

3. EXPERIMENT

In order to reduce the relative error δ_λ of the obtained wavelength values for individual modes of standing wave oscillation, we made some changes to the algorithm we implemented in Mathematica. In an algorithm that required minimal deviation of the obtained wavelength from its exact value for different standing wave modes, we changed the length of the side of the L_y to be variable. In effect, the program searched the values of standing wave modes and found the width at which the deviation was minimal. The width of the oven interior was chosen to be of variable size, because it was easiest to change it in a real experiment by reducing the width. This was achieved by placing a reflector (stainless steel sheet, 1mm thick) on the opposite side of the magnetron - parallel to its opposite side. Figure 6 shows a flowchart of the algorithm for finding the optimum width of square-shaped resonators (microwave oven interior), for transverse electromagnetic waves.

Table 2 shows the modes that exhibited the smallest relative wavelength error, for the interval of the interior width of the microwave from $L_y/2$ to L_y = 29.5 cm.

Table 2. *Wavelengths λ_d whose values were closest to the wavelength of magnetron radiation, their relative errors and obtained oscillation modes, for the microwave oven dimensions L_x = 25.5 cm, L_z = 18.1 cm and variable width L_y*

λ_d (cm)	δ_λ (%)	L_y (cm)	*l*	m	n
12.238	0.016	27.9	2	4	0
12.240	0.029	26.5	1	3	2
12.239	0.021	22.7	2	3	1
12.237	0.009	21.8	4	1	0
12.233	0.028	21.7	4	1	0
12.233	0.029	20.2	3	2	1

Based on Table 2, by reducing the internal width of the L_y oven by 3 cm, the resulting relative error for δ_λ (mod $TE_{1,3,2}$) can be significantly reduced, thereby significantly contributing to the proper formation of standing wave modes.

After this correction, shortening of L_y to 26.5 cm, an experiment was carried out in which an organic mixture (wax and chocolate bar) was placed in the xy-plane at a height of z_0 = 2.5 cm and subjected to electromagnetic radiation for 2 min at medium intensity, where z_0 was the distance from the bottom of the oven to the upper surface of the body that was placed inside.

After the experiment, the distance between the anti-nodes of the standing wave were measured (Figure 7).

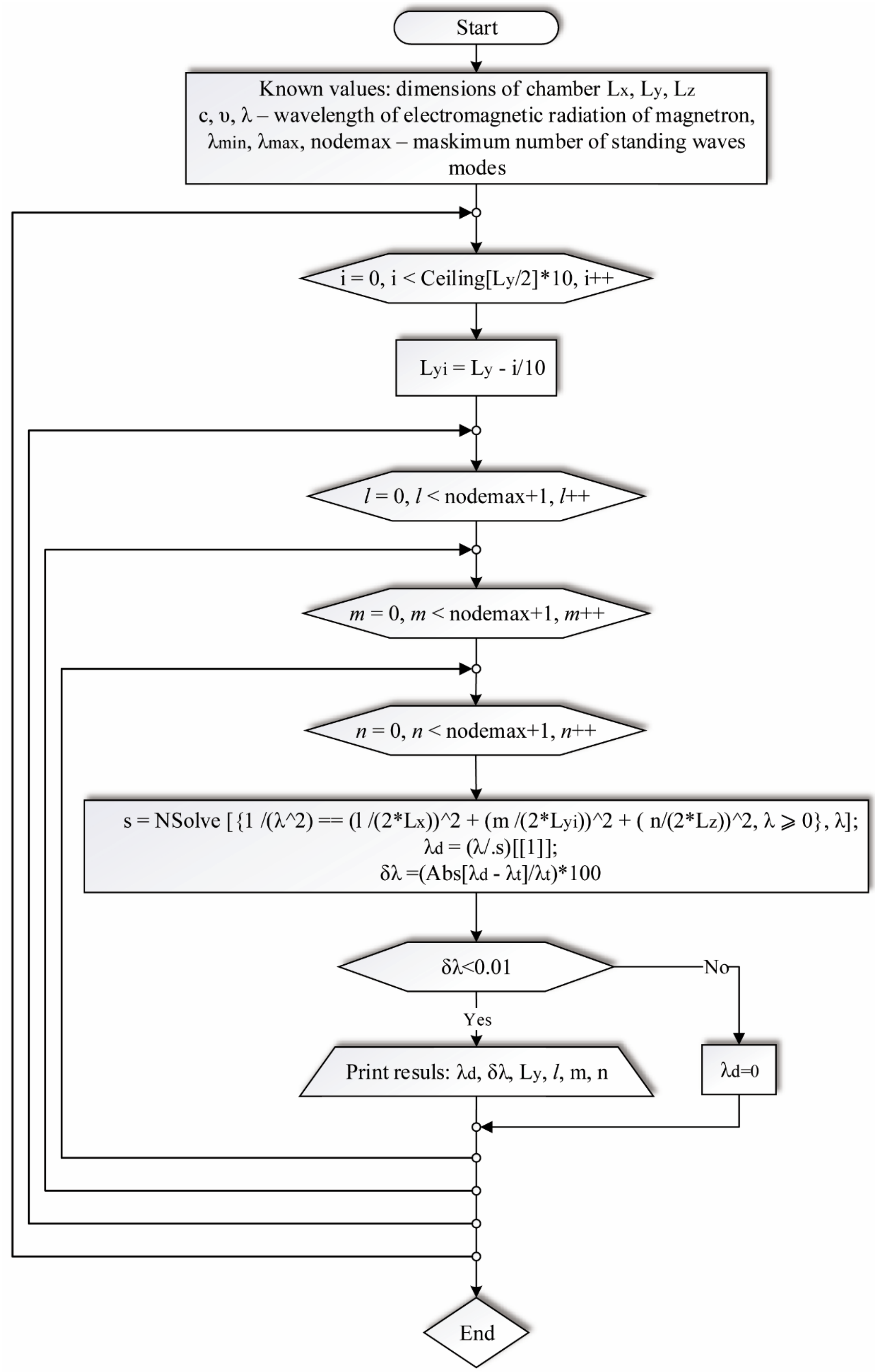

***Figure 6**. Flowchart of algorithm for finding the optimal width of the 3D resonator*

4. RESULTS AND DISCUSSION

When the distance between the centers of the anti-nodes of the standing wave was measured, it was noticed that they did not lie in a plane parallel to the horizontal plane, but were at a certain angle α relative to it. We came to this conclusion by observing the width and depth of the anti-nodes whose diameters were not the same, although this could be expected from the proper formation of modes. Therefore, it was necessary to make additional calculations to determine the positions of the centers of the anti-nodes $O_1(x_1,y_1,z_1)$ and $O_2(x_2,y_2,z_2)$ in the 3D space and the distance between them $\overline{O_1O_2}$ (Fig. 8).

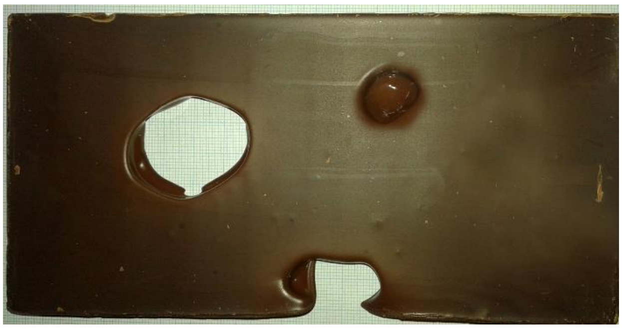

Figure 7. *"Imprint" of the anti-nodes of the standing wave on a chocolate bar at a height of z_0 = 2.5 cm*

The measurements were made of the widths (L_1, L_2 - circle chords), and the depth (d_2) of the melted part of the body (hot-spots) exposed to radiation, as well as their center distances (D_{xy}). The depth d_1, which is slightly larger than d_2, was obtained by calculations.

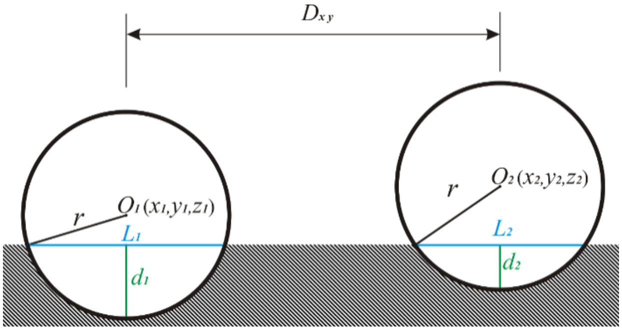

Figure 8. *Schematic representation of the anti-nodes of the standing waves (spheres with centers in O_1 and O_2), in relation to the body exposed to electromagnetic radiation*

The reason for this was that in a certain number of measurements, depth d1 was greater than the thickness of the body exposed to electromagnetic radiation (wax or other substance). The radius, *r,* of the sphere was calculated based on the obtained data. Then d_1 was calculated assuming that *r* of both spheres was the same. Table 3 shows measured values.

Figure 9 shows a hot-spot (anti-node) of standing waves with radius *r*, presented through a projection in 2D space.

Table 3. *Measured parameters of standing wave anti-nodes*

First anti-node		Second anti-node		Distance of centers
d_1 (mm)	L_1 (mm)	d_2 (mm)	L_2 (mm)	D_{xy} (mm)
16.74	38.3	2,5	19	59.7

The size of the radius spheres (i.e. the circle) *r*, depends on the duration and intensity of electromagnetic radiation.

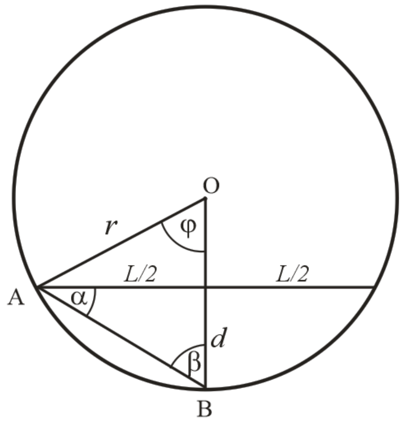

Figure 9. *Sketch of the hot-spot of the standing wave - circle with center at point O*

It is apparent in Figure 9 that the line $\frac{L}{2}$, which originates at point A and is normal to line BO, can be written as $\frac{L}{2} = r\sin\varphi$. It follows that

$$r = \frac{L}{2\sin\varphi} \tag{8}$$

Also, Figure 9 shows that angles α and β are $\alpha = \frac{\varphi}{2}$, $\beta = \frac{\pi}{2} - \frac{\varphi}{2}$, so

$$\tan\frac{\varphi}{2} = \frac{d}{\frac{L}{2}} = \frac{2d}{L} \tag{9}$$

, and it follows that

$$\varphi = 2\tan^{-1}\frac{2d}{L} \tag{10}$$

It is obvious that for $x > 0$

$$\tan^{-1}\frac{1}{x} = \frac{\pi}{2} - \tan^{-1}x \tag{11}$$

and the change $x = \frac{L}{2d}$ results in

$$\tan^{-1}\frac{2d}{L} = \frac{\pi}{2} - \tan^{-1}\frac{L}{2d} \tag{12}$$

, or

$$2\tan^{-1}\frac{2d}{L} = \pi - 2\tan^{-1}\frac{L}{2d} \tag{13}$$

By substituting equation (13) in equation (10), we have that angle φ

$$\varphi = \pi - 2\tan^{-1}\frac{L}{2d} \tag{14}$$

Replacing the last expression in equation (8) yields

$$r = \frac{L}{2\sin\left(\pi - 2\tan^{-1}\frac{L}{2d}\right)} = \frac{L}{2\sin\left(2\tan^{-1}\frac{L}{2d}\right)} \tag{15}$$

The last equation is crucial for the tomographic reconstruction of the mutual positions of the hot-spots of the standing wave. It correlates the radius of the circle (or sphere), that is, the anti-node of the standing wave *r*, its circle chord *L* and the distance of the center of the circle chord from the circle *d*.

Since D_{xy} is given by

$$D_{xy} = \sqrt{\left(\Delta x^2\right) - \left(\Delta y^2\right)} = \sqrt{\left(x_2 - x_1\right)^2 - \left(y_2 - y_1\right)^2} \tag{16}$$

, and the distance between the centers O_1 and O_2 by

$$\overline{O_1O_2} = \sqrt{\left(\Delta x^2\right) + \left(\Delta y^2\right) + \left(\Delta z^2\right)} \tag{17}$$

we have

$$\overline{O_1O_2} = \sqrt{D_{xy}^2 + \left(\Delta z\right)^2} = \sqrt{D_{xy}^2 - \left(z_2 - z_1\right)^2} \tag{18}$$

where $z_1 = z_0 - d_1 + r_1$, $z_2 = z_0 - d_2 + r_2$ and $r_1 = r_2$. From there Δz becomes

$$\Delta z = z_2 - z_1 = z_0 - d_2 + r - z_0 + d_1 + r = d_1 - d_2 \tag{19}$$

, so the distance between the centers O_1 and O_2 is

$$\overline{O_1O_2} = \sqrt{D_{xy}^2 + \left(\Delta d\right)^2} \tag{20}$$

Angle α between the level of the hot-spots of the standing wave and the horizontal plane is given as

$$\alpha = \cos^{-1}\left(\frac{D_{xy}}{\overline{O_1O_2}}\right) \tag{21}$$

Using the data from Table 3, we obtained $\overline{O_1O_2}$= 61.37 mm and α = 13.4° which represents λ/2 of electromagnetic waves within the oven. Based on these data, our calculation gives the value of the frequency of the electromagnetic wave of the emitted radiation $\upsilon = 2.443\cdot10^9$ Hz. This represents a deviation of 0.3% for frequency υ_0 and the same deviation is obtained for the wavelength of magneton radiation λ_0.

5. CONCLUSION

From the experiment described in the paper we learned that small changes in the dimensions of the resonators can results in the formation of certain modes of standing wave. An algorithm was proposed to help find the optimal dimensions of 3D space, as well as the standing wave modes that would arise in such a space.

The anti-nodes of the standing wave are in a plane aligned with some angle α to the plane of the bottom of the microwave oven. With a tomographic projection of the distance of the hot-spots, it is possible to reconstruct their positions in the oven interior.

With this type of experiment it is possible to draw conclusions in a way that could be interesting to students, about various physical phenomena and the relationships between individual physical quantities that describe the given phenomena.

REFERENCES

[1] V. Surducan, E. Surducan, R. Ciupa, and C. Neamtu, "Microwave generator for scientific and medical applications," in *AIP Conference Proceedings*, 2012, vol. 1425, pp. 89–92.

[2] V. Michael, K.-P. Möllmann, and D. Karstädt, "More experiments with microwave ovens," *Phys. Educ.*, vol. 39, no. 4, pp. 346–351, 2004.

[3] M. Vollmer, K.-P. Möllmann, and D. Karstädt, "Microwave oven experiments with metals and light sources," *Phys. Educ.*, vol. 39, no. 6, pp. 500–508, 2004.

[4] A. C. Scott, *Encyclopedia of nonlinear science*. 2005.

[5] S. Kamol, P. Limsuwan, and W. Onreabroy, "Three-dimensional standing waves in a microwave oven," *Am. J. Phys.*, vol. 78, no. 5, p. 492, 2010.

[6] J. Brody, E. Villhauer, and H. Espiritu, "Standing waves between a microwave transmitter and receiver The motion of a ball moving down a circular path Standing waves between a microwave transmitter and receiver," *Am. J. Phys.*, vol. 821, no. 10, 2014.

[7] A. Steyn-Ross and A. Riddell, "Standing waves in a microwave oven," *Phys. Teach.*, vol. 28, no. 7, pp. 474–476, 1990.

[8] D. A. Copson and R. V. Decareau, *Microwave Power Engineering*. Academic, New York, 1968.

[9] M. Vollmer, "Physics of the microwave oven," *Phys. Educ.*, vol. 39, no. 1, pp. 74–81, 2003.

[10] M. Lukovic, V. Lukovic, I. Belca, B. Kasalica, I. Stanimirovic, and M. Vicic, "LED-based Vis-NIR spectrally tunable light source - the optimization algorithm," *J. Eur. Opt. Soc.*, vol. 12, no. 1, 2016.

[11] M. Sadaghdar, "Speed of Light, Microwave Oven and How It Works," 2017. [Online]. Available: https://www.youtube.com/watch?v=nqTDCkuVADw.